Eur J Nucl Med Mol Imaging (2010) 37:1950–1958
DOI 10.1007/s00259-010-1489-y

ORIGINAL ARTICLE

Biodistribution and radiation dosimetry of ^{11}C-labelled docetaxel in cancer patients

Astrid A. M. van der Veldt · N. Harry Hendrikse · Egbert F. Smit · Martien P. J. Mooijer · Anneloes Y. Rijnders · Winald R. Gerritsen · Jacobus J. M. van der Hoeven · Albert D. Windhorst · Adriaan A. Lammertsma · Mark Lubberink

Received: 30 November 2009 / Accepted: 27 April 2010 / Published online: 27 May 2010

Abstract
Purpose Docetaxel is an important chemotherapeutic agent used for the treatment of several cancer types. As radiolabelled anticancer agents provide a potential means for personalized treatment planning, docetaxel was labelled with the positron emitter ^{11}C. Non-invasive measurements of [^{11}C]docetaxel uptake in organs and tumours may provide additional information on pharmacokinetics and pharmacodynamics of the drug docetaxel. The purpose of the present study was to determine the biodistribution and radiation absorbed dose of [^{11}C]docetaxel in humans.
Methods Biodistribution of [^{11}C]docetaxel was measured in seven patients (five men and two women) with solid tumours using PET/CT. Venous blood samples were collected to measure activity in blood and plasma. Regions of interest (ROI) for various source organs were defined on PET (high [^{11}C]docetaxel uptake) or CT (low [^{11}C]docetaxel uptake). ROI data were used to generate time-activity curves and to calculate percentage injected dose and residence times. Radiation absorbed doses were calculated according to the MIRD method using OLINDA/EXM 1.0 software.
Results Gall bladder and liver demonstrated high [^{11}C]docetaxel uptake, whilst uptake in brain and normal lung was low. The percentage injected dose at 1 h in the liver was 47±9%. [^{11}C]docetaxel was rapidly cleared from plasma and no radiolabelled metabolites were detected. [^{11}C]docetaxel uptake in tumours was moderate and highly variable between tumours.
Conclusion The effective dose of [^{11}C]docetaxel was 4.7 μSv/MBq. As uptake in normal lung is low, [^{11}C]docetaxel may be a promising tracer for tumours in the thoracic region.

Keywords [^{11}C]docetaxel · Biodistribution · Radiation dose · Cancer · PET/CT

A. A. M. van der Veldt (✉) · N. H. Hendrikse · M. P. J. Mooijer · A. Y. Rijnders · A. D. Windhorst · A. A. Lammertsma · M. Lubberink
Department of Nuclear Medicine & PET Research,
VU University Medical Center,
P.O. Box 7057, 1007 MB Amsterdam, The Netherlands
e-mail: aam.vanderveldt@vumc.nl

N. H. Hendrikse
Department of Clinical Pharmacology & Pharmacy,
VU University Medical Center,
Amsterdam, The Netherlands

E. F. Smit
Department of Pulmonology, VU University Medical Center,
Amsterdam, The Netherlands

W. R. Gerritsen
Department of Medical Oncology, VU University Medical Center,
Amsterdam, The Netherlands

J. J. M. van der Hoeven
Department of Internal Medicine, Medical Center Alkmaar,
Alkmaar, The Netherlands

Introduction

Tumour resistance to chemotherapy remains a major challenge, because it results in unnecessary toxicity and costs and, most importantly, delay in initiating potentially more effective treatment. In the last decade, there has been growing interest in molecular imaging for tumour response monitoring at an early stage during treatment. For example, glucose metabolism as measured by the commonly used positron emission tomography (PET) tracer 2-[^{18}F]fluoro-2-deoxy-D-glucose ([^{18}F]FDG) has been accepted as a

surrogate end-point for the evaluation of new drugs in oncology [1]. However, [^{18}F]FDG PET can only measure tumour response after treatment has already been started by comparing a response scan with the corresponding baseline scan. Ideally, response to anticancer drugs should be predicted before initiating therapy. Anticancer agents that are labelled with a positron emitter may be promising tracers for predicting treatment outcome before initiating treatment [2]. A few studies have suggested that radiolabelled anticancer agents may provide a unique means for personalized treatment planning in cancer patients [2], but more studies are needed to substantiate this concept. In addition, radiolabelled anticancer agents may contribute to drug development and the rational development of combination therapy strategies by exploring whether drug pharmacokinetics can be modulated by other agents. The anticancer drug docetaxel has been radiolabelled with ^{11}C [3–5]. Docetaxel belongs to the taxanes, one of the most active classes of cytotoxic agents, and has been approved for the treatment of several cancer types, including breast, prostate and lung cancer [6]. Docetaxel acts by disrupting the microtubular network which results in the inhibition of mitosis in cells. In spite of this effective mechanism of action in tumours, the efficacy of docetaxel treatment in cancer patients is not optimal. Appropriate selection of patients and addition of biomodulating agents may improve efficacy of docetaxel therapy. PET using [^{11}C]docetaxel may be valuable, as it allows for measurement of docetaxel uptake in tumours and for investigating effects of other agents on this uptake. In preparation for kinetic studies in cancer patients, the purpose of the present study was to determine biodistribution and radiation absorbed doses of [^{11}C]docetaxel in humans.

Materials and methods

Patients

Patients with advanced solid tumours, due to undergo chemotherapy, were eligible for this study. Inclusion criteria were: 18 years of age or older, malignant lesion of at least 1.5 cm in diameter within the chest as measured by Response Evaluation Criteria in Solid Tumors (RECIST) [7], life expectancy of at least 12 weeks, Karnofsky performance status scale>60%, platelets>100×10^9/l and haemoglobin> 6.0 mmol/l. Exclusion criteria included previous treatment with taxanes, claustrophobia, pregnant or lactating patients, patients having metal implants (e.g. pacemakers), use of coumarin derivatives or inhibitors of platelet aggregation, use of drugs that are inhibitors of or substrates for P-glycoprotein (Pgp), concurrent treatment with experimental drugs and participation in a clinical trial with any investigational drug within 30 days prior to study entry. The study was approved by the Medical Ethics Review Committee of the VU University Medical Center. Five male and two female patients with a mean age (± SD) of 63± 10 years and a mean body weight (± SD) of 78±15 kg (range: 66–94 kg) were included in the study. All patients were diagnosed with metastatic cancer including non-small cell lung cancer (NSCLC) (n=5), malignant pleural mesothelioma (n=1) and prostate cancer (n=1). Prior to inclusion, each patient signed a protocol-specific informed consent.

Synthesis of [^{11}C]docetaxel

[^{11}C]docetaxel was synthesized according to Good Manufacturing Practice (GMP) standards as described in detail previously [4, 5]. For the preparation of the precursor, the drug docetaxel was obtained from Green Plantchem Company Ltd. (Hangzhou, China). Briefly, the ^{11}C isotope was introduced in the side chain by a [^{11}C]*tert*-butoxycarbonylation of the free amine of docetaxel, and [^{11}C]docetaxel was produced with a decay-corrected overall radiochemical yield of 10±1% prior to purification. The mean specific activity at time of injection was 7±5 GBq/μmol.

Scan protocol

Patients were asked to fast over midnight before scanning. A light breakfast before 8.00 a.m. and water and tea were allowed. Due to the fact that only sub-pharmacological (tracer) doses of [^{11}C]docetaxel were administered, no side effects were expected. The Medical Ethics Review Committee, however, required that dexamethasone be given to prevent potential allergic reactions. Two dosages of 4 mg dexamethasone were given; one in the evening and the other in the morning before [^{11}C]docetaxel administration. Whole-body scans were performed on a Gemini TF-64 PET/CT scanner (Philips Medical Systems, Best, The Netherlands) [8]. Each patient was positioned on the scanner bed using elastic body-restraining bandages to minimize body movement during the scans. Following a 50 mAs low-dose CT (LD-CT) scan, a mean (± SD) single bolus of 178±79 MBq [^{11}C]docetaxel (dissolved in a maximum volume of 12 ml saline) was injected intravenously and four serial whole-body PET scans from head to mid-thigh were acquired over a 1-h period with progressive increase of scan durations per bed position of 0.5, 1, 1.5 and 2 min, respectively. The axial field of view of the scanner is 18 cm and a 50% overlap between bed positions is applied in whole-body scans, resulting in an average of 11 bed positions per scan. Resulting mean durations of the four consecutive whole-body PET scans were 6.9±1.2, 12.6±2.3, 18.3±3.3 and 24.0±4.3 min, respectively. One patient was able and willing to undergo a fifth whole-body

scan with duration of 2.5 min per bed position. Data was normalized and all appropriate corrections were applied for dead time, randoms, scatter, attenuation and scanner calibration, and whole-body scans were corrected for decay relative to the start of each scan. Images were reconstructed using time-of-flight ordered subsets expectation maximization (TF-OSEM).

Analysis of blood samples

After each whole-body scan, a venous blood sample (7 ml) was collected for measuring blood and plasma concentrations as well as radiolabelled metabolites. To avoid contamination of activity remaining in the catheter, 3–5 ml blood was withdrawn prior to each sample and the line was flushed with 2 ml saline after sampling, as described previously [9]. A cross-calibrated gamma counter was used to determine activity concentrations and plasma to whole blood ratios. The presence of radiolabelled metabolites in plasma was assessed using solid phase extraction (SPE) combined with high-performance liquid chromatography (HPLC) using offline detection.

Region of interest definition

PET and LD-CT images were converted to ECAT 7 format and regions of interest (ROIs) were drawn using CAPP software (CTI/Siemens, Knoxville, TN, USA) to obtain mean activity concentration in each region at each of the four time points. For organs with activity concentrations clearly exceeding background levels [liver, gall bladder, upper large intestine (ULI), urinary bladder, heart wall, bone marrow in vertebrae], ROIs were defined on the PET scan with the highest tracer uptake (Fig. 1) using a 50% isocontour. For organs with lower tracer uptake (brain, lung, spleen, kidney) that could easily be identified on the LD-CT scan, ROIs were drawn manually on the LD-CT scan and subsequently copied to the PET scans (Fig. 2). For each patient, a ROI of one tumour of at least 1.5 cm in diameter that could easily be identified on the LD-CT scan was determined. All ROIs were projected onto all scans. As the volume of the urinary bladder increased during scanning, bladder ROIs were separately drawn on each PET image except for the first image. The bladder ROI of the second image was projected onto the first PET scan.

Calculation of [^{11}C]docetaxel uptake

ROIs were used to generate time-activity curves (TAC) for each source organ. The time of measurement of each individual organ in each scan was calculated based on the organ position in the whole-body image and the total duration of that scan. All organ TACs were then corrected for decay relative to the time of injection of the tracer. To assess biodistribution, the mean standardized uptake value (SUV) normalized to body weight and the percentage injected dose (%ID) in each organ were calculated at each time point. For organs with ROIs covering less then the entire organ (ULI, myocardial wall, red marrow), the percentage of injected activity per cm^3 was multiplied with the organ volumes of the adult male reference phantom, scaled with the ratio of the patient's weight and the reference man weight [10, 11]. Since bones not containing active marrow were not visible in the images, all activity in vertebrae ROIs was assumed to be in red marrow. For tumours, the maximum SUV (SUV_{max}) was calculated.

Residence time and absorbed dose calculations

For each organ, TACs were uncorrected for decay and residence times were computed as the trapezoidal sum of the TAC with the assumption that, after the last time point, activity decreased only by physical decay (i.e. no biological clearance after the last time point). Residence time for the remainder of the body was calculated as the total body residence time without voiding (one divided by the decay constant) minus the sum of the residence times of all defined organs. Residence times for each patient were

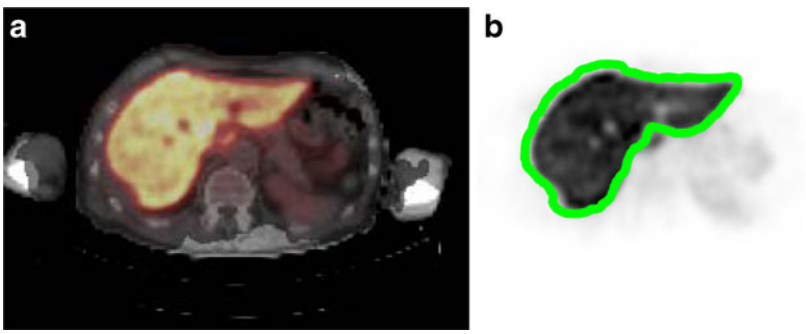

Fig. 1 For organs with activity clearly exceeding background (e.g. liver) ROIs were defined on the PET scan with the highest uptake. PET/CT fusion image (**a**) and PET image (**b**) demonstrate high [^{11}C] docetaxel uptake in liver. The liver ROI as determined on the PET image is presented in *green* (**b**)

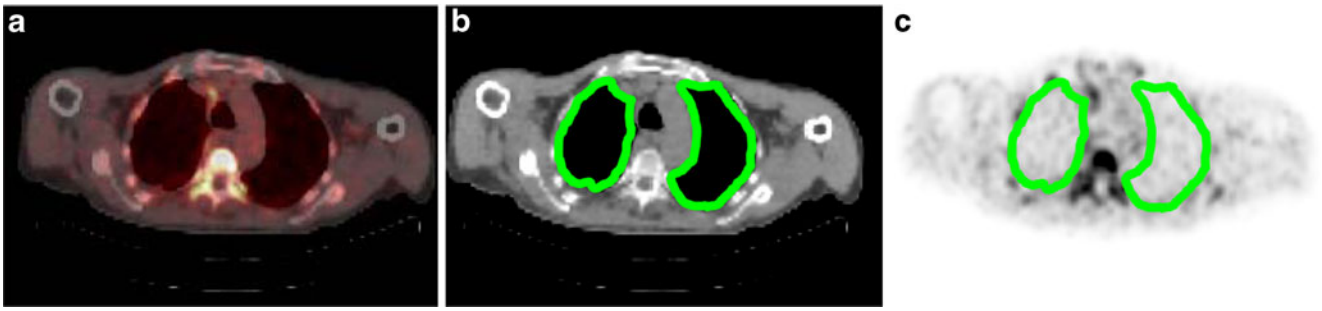

Fig. 2 For organs with lower tracer uptake (e.g. lung), ROIs were drawn on the LD-CT scan and subsequently copied onto the PET scans. PET/CT fusion image (**a**) and PET image demonstrate low [^{11}C]docetaxel uptake in lungs. The lung ROIs were drawn on the CT image (**b**) and projected onto the PET image (**c**). The lung ROIs as determined on the LD-CT scan are presented in *green* (**b**, **c**)

entered into the OLINDA/EXM 1.0 software package [12] to compute absorbed doses using the adult male reference phantom. Since the small intestine (SI) was difficult to delineate in both PET and LD-CT images due to the vicinity to the liver and the poor contrast of the LD-CT images, the ICRP 30 GI [13] tract model was used to estimate residence times in SI and lower large intestine (LLI) based on those found for ULI. According to this model, ratios of SI to ULI and LLI to ULI residence times are 8.45 and 0.039, respectively, for ^{11}C-labelled tracers [12]. OLINDA/EXM 1.0 provides effective dose values according to ICRP 60 [14] and does not provide effective dose values according to the latest definition (ICRP 103, [15]). Therefore, effective doses according to ICRP 103 were calculated manually using target organ doses as reported by OLINDA/EXM 1.0 and ICRP 103 weighting factors. Since not all target organs are included in OLINDA/EXM 1.0 (skin, salivary glands, oesophagus), the sum of weighting factors was 0.94 and effective dose values were divided by 0.94 [16].

Results

Biodistribution

Figure 3 shows the typical biodistribution of [^{11}C]docetaxel over time, as obtained from the four sequential PET acquisitions over about 1 h. Liver, gall bladder, intestine and urinary bladder were visually identified as organs with relatively high activity, whilst [^{11}C]docetaxel uptake in brain and normal lung was low. Between the third and fourth PET scans, [^{11}C]docetaxel uptake in gall bladder and intestine was still increasing. Figure 4 shows TACs for various organs [%ID versus time post-injection (p.i.)]. Percentage ID at 1 h p.i. was highest in liver (47±9%) and gall bladder (7.2±3.6%), with 35% of all disintegrations occurring in the liver. The highest peak activity concentrations were measured in gall bladder (SUV_{mean} 96±49), liver (SUV_{mean} 24±3) and ULI (SUV_{mean} 9±6), whereas concentrations were smallest in brain (SUV_{mean} 0.05±0.03) and lung (SUV_{mean} 0.7±0.2).

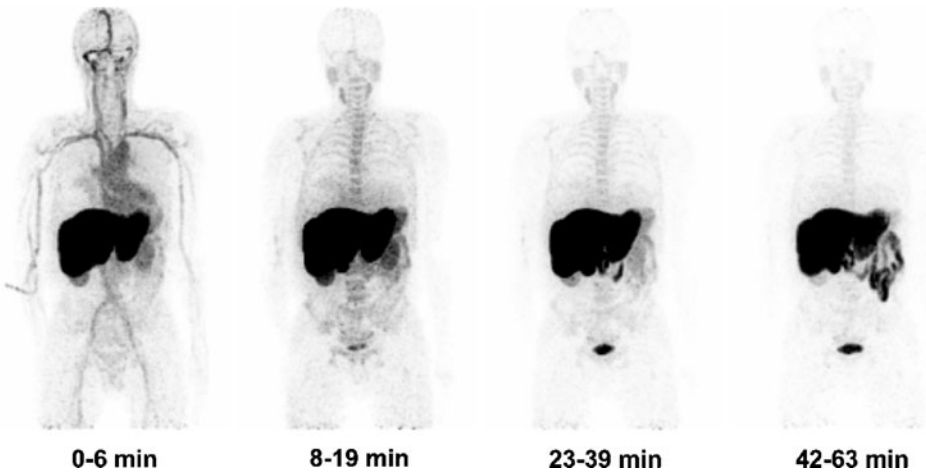

Fig. 3 Maximum intensity projections of the biodistribution of [^{11}C]docetaxel in a 71-year-old male patient with metastatic malignant pleural mesothelioma. The four successive whole-body PET scans (0–6, 8–19, 23–39 and 42–63 min p.i.) demonstrate high liver uptake at all time points and low uptake in brain and normal lung. On the fourth scan, [^{11}C]docetaxel uptake is observed in intestine

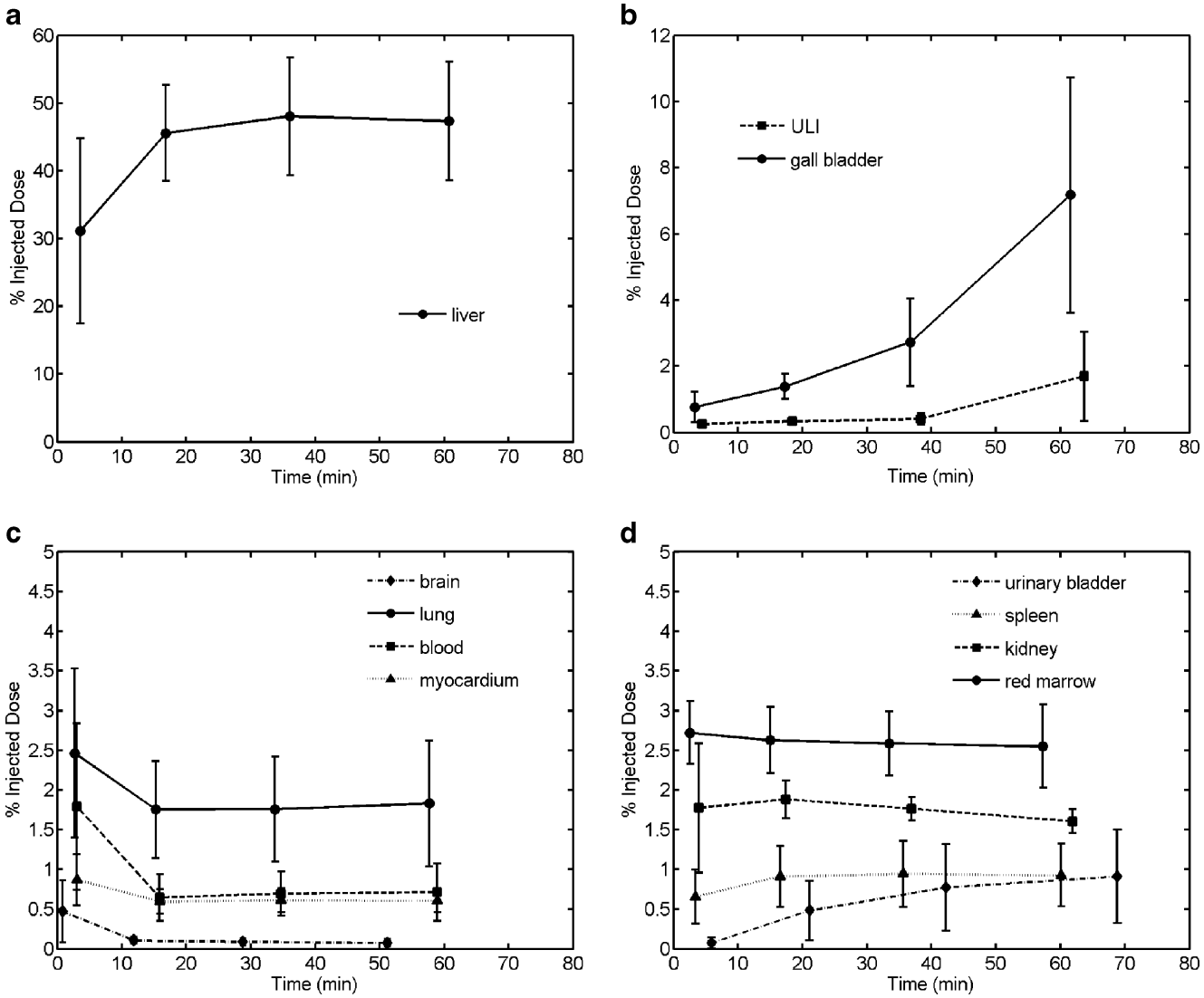

Fig. 4 Decay-corrected TACs of [^{11}C]docetaxel (%ID versus time p.i.) (n=7) in **a** liver, **b** ULI and gall bladder, **c** brain, lung, heart contents and myocardial wall, and **d** urinary bladder, spleen, kidney and red marrow. *Vertical bars* indicate standard deviation

Blood clearance

[^{11}C]docetaxel was rapidly cleared from the blood pool and within 30 min %ID/ml was less than 0.001, as shown in Fig. 5. After the first PET scan, plasma values were higher than those of whole blood, but after the second scan and onwards whole blood values were higher. No radiolabelled metabolites were detected in plasma, with the HPLC chromatogram showing a single peak due to [^{11}C]docetaxel itself. Recovery of radioactivity in the HPLC analysis was 94±5%.

Safety

Patients did not report any side effect or discomfort after the [^{11}C]docetaxel injection and during the imaging procedure.

Radiation dosimetry

Table 1 summarizes average organ residence times calculated from the whole-body images of the seven patients. Organ absorbed dose estimates are displayed in Table 2. Estimated radiation absorbed doses were highest in liver and gall bladder wall at 35.2±6.6 and 34.6±9.9 μGy/MBq, respectively. Based on these results, the mean effective dose for [^{11}C]docetaxel was estimated at 4.7±0.2 μSv/MBq.

Tumour uptake

[^{11}C]docetaxel uptake was observed in tumours. Figure 6 shows a patient with [^{11}C]docetaxel uptake in a mediastinal metastasis of a malignant pleural mesothelioma. In each patient, one tumour was selected for further analysis, consisting of primary NSCLC (n=3), mediastinal lymph

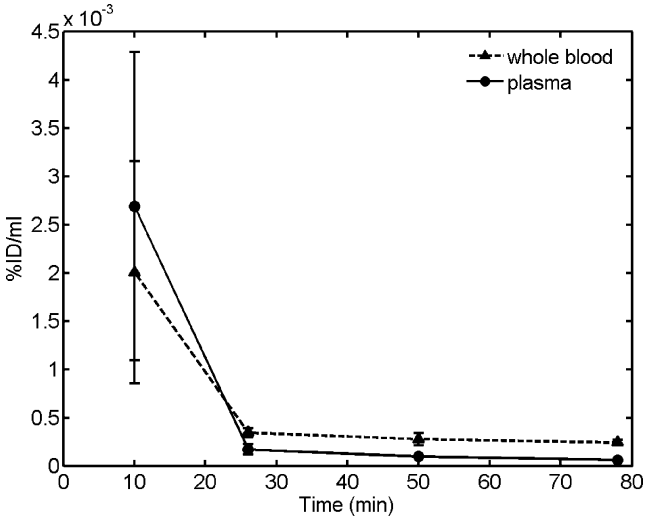

Fig. 5 Decay-corrected TACs of [^{11}C]docetaxel (%ID/ml versus time p.i.) in plasma and whole blood

node metastasis of NSCLC (n=1), supraclavicular lymph node metastasis of NSCLC (n=1), mediastinal lymph node metastasis of malignant pleural mesothelioma (n=1) and lung metastasis of prostate cancer (n=1).The TACs for these seven tumours are shown in Fig. 7. The highest measured SUV_{max} was 5.1.

Discussion

In the present study, the biodistribution of [^{11}C]docetaxel was measured in seven patients with metastatic solid tumours using whole-body PET/CT scans, and radiation absorbed doses were estimated. The LD-CT scan was of additional value to identify organs with low [^{11}C]docetaxel uptake. Uptake of [^{11}C]docetaxel appeared to be highest in gall bladder and liver, whilst uptake in normal lung and brain was very low. Furthermore, [^{11}C]docetaxel uptake in tumours was moderate and highly variable between different tumours. The results of the present study showed promising biodistribution and radiation dosimetry of [^{11}C]docetaxel. For a typical administration of 370 MBq [^{11}C]docetaxel, the estimated dose is 1.7 mSv, which is within the 1–10 mSv range of effective doses that are acceptable for volunteers in biomedical research [17]. The tracer was rapidly cleared from the blood pool which resulted in images of high quality and reliable statistics for quantification. The main route of elimination of the tracer was the hepatobiliary pathway which contributed to a relatively high radiation burden to gall bladder and liver. During the successive PET scans, extensive hepatic uptake and subsequent excretion into gall bladder and intestine were observed (Fig. 3). The SUV_{mean} of [^{11}C]docetaxel was highest in gall bladder, which is also the dose-limiting organ for [^{11}C]docetaxel. For an administration of 370 MBq, the

Table 1 Average (± SD) organ residence times for [^{11}C]docetaxel uptake (n=7)

Organ	Organ residence time (h)
Brain	0.0008±0.0003
Gall bladder	0.0124±0.0045
Small intestine	0.0243±0.0133
Upper large intestine	0.0029±0.0016
Lower large intestine	0.0001±0.0001
Heart contents	0.0046±0.0016
Heart wall	0.0032±0.0006
Kidney	0.0085±0.0016
Liver	0.2047±0.0401
Lung	0.0095±0.0038
Red marrow	0.0128±0.0018
Spleen	0.0041±0.0015
Urinary bladder	0.0023±0.0015
Remainder of body	0.2002±0.0421

Table 2 Radiation absorbed dose estimates for [^{11}C]docetaxel

Target organ	μGy/MBq (mean±SD)
Adrenals	4.1±0.2
Brain	0.5±0.1
Breast	1.6±0.1
Gall bladder wall	34.6±9.9
Lower large intestine wall	2.1±0.3
Small intestine	9.5±3.8
Stomach	2.6±0.1
Upper large intestine wall	5.1±1.2
Heart wall	6.0±1.0
Kidney	10.7±1.5
Liver	35.2±6.6
Lung	4.1±1.0
Muscle	1.9±0.2
Ovary	2.4±0.3
Pancreas	4.0±0.1
Red marrow	3.2±0.2
Bone surface	3.1±0.3
Skin	1.3±0.2
Spleen	7.4±2.3
Testis	1.3±0.3
Thymus	1.8±0.2
Thyroid	1.4±0.3
Urinary bladder wall	3.1±1.1
Uterus	2.3±0.3
Total body	2.9±0.0
Effective dose (μSv/MBq)	4.7±0.2

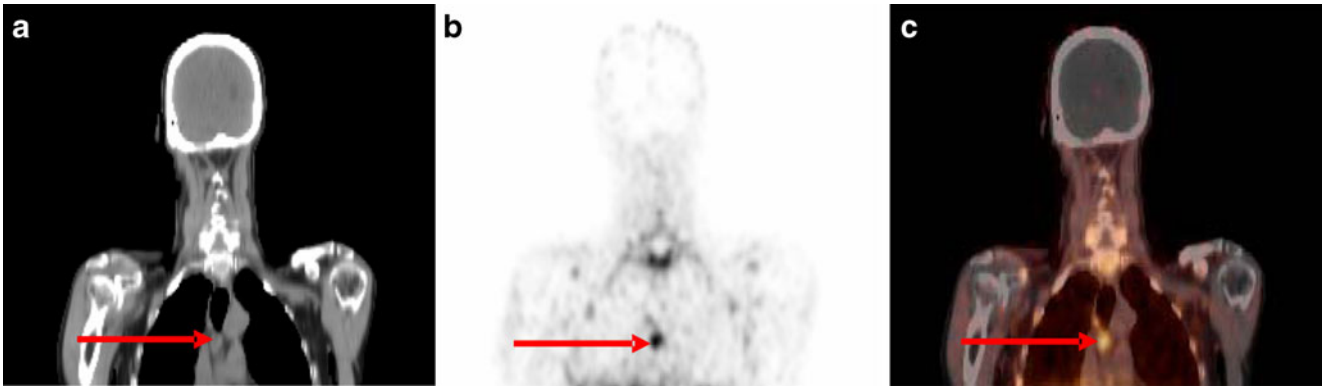

Fig. 6 PET/CT images of [^{11}C]docetaxel in a 71-year-old male patient with metastatic malignant pleural mesothelioma. Mediastinal metastasis (*arrow*) on CT scan (**a**) with [^{11}C]docetaxel uptake on PET scan (**b**) and on PET/CT fusion image (**c**)

absorbed dose to the gall bladder wall is 12.8±3.7 mGy. This equals 26% of the maximum allowed dose of 50 mGy to a single organ for a single administration to an adult research subject [18]. The high liver uptake of [^{11}C] docetaxel suggests extensive metabolism of the tracer. The fact that no radioactive metabolites were measured in plasma shows that if radioactive metabolites are produced, none of these enter the bloodstream during the course of the PET scan and, consequently, none are transported to tumours. In fact, radioactivity was nearly completely cleared from plasma within the first 20 min. This does not rule out the presence of re-circulating non-radiolabelled metabolites in plasma, as has been observed in earlier studies with therapeutic doses of cold docetaxel [19].

Uptake in all organs except gall bladder and ULI reached a plateau within 10 min after injection, after which %ID remained nearly constant during the rest of the scan. Therefore, further clearance according to physical decay only appears to be a valid assumption. During the fourth PET scan (~60 min after injection), uptake in gall bladder and ULI was still increasing, indicating that the absorbed dose of [^{11}C]docetaxel in gall bladder and intestine might be underestimated. In the patient who underwent a fifth whole-body scan, however, gall bladder and ULI uptake decreased rapidly during the last scan. Inclusion of this fifth scan resulted in a decreased effective dose (4.0 vs 4.1 mSv/MBq), although giving a small increase in absorbed dose to the gall bladder (Fig. 8). This indicates that exponential extrapolation according to physical decay after the fourth measurement yields conservative effective dose values. The use of more and faster whole-body scans within the first hour after injection, as has been published for similar studies with other tracers [20, 21], would not have led to major differences in the results because of the near constant uptake in most organs.

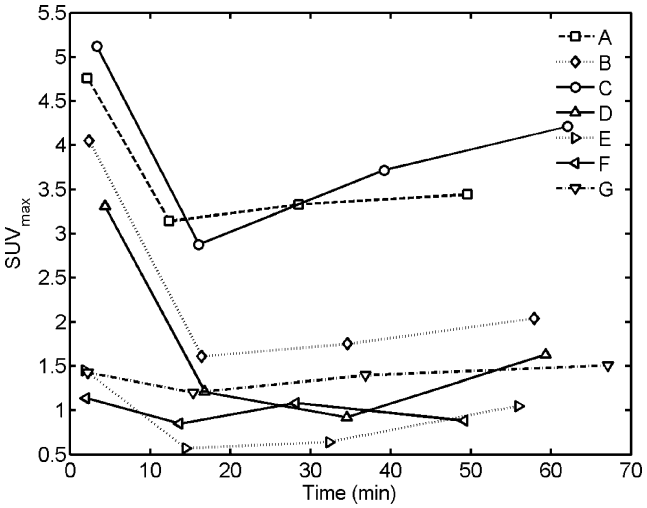

Fig. 7 Decay-corrected TACs of [^{11}C]docetaxel for seven different tumours (SUV_{max} versus time p.i.) including mediastinal metastasis of malignant pleural mesothelioma (**a**), metastasis of NSCLC (**b**, **d**), primary tumour of NSCLC (**c**, **e**, **f**) and lung metastasis of prostate cancer (**g**)

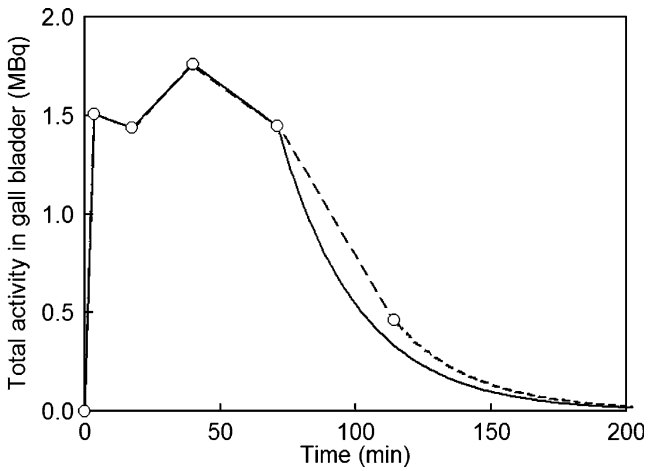

Fig. 8 Total activity (non-decay-corrected) in gall bladder in a single patient who underwent an additional fifth whole-body scan. *Solid lines* show the interpolated data from which the trapezoidal integral was computed, assuming physical decay after the fourth whole-body scan, whereas *dashed lines* show the integral after inclusion of the fifth whole-body scan

As most anticancer agents are eliminated by liver, extensive hepatic clearance and subsequent excretion into the gall bladder and intestine may also be expected for other radiolabelled anticancer drugs. Due to the resulting high background and low contrast in the abdomen, the value of these radiolabelled anticancer drugs for tumours in the abdominal and pelvic region may be limited.

Paclitaxel, another taxane, has been radiolabelled with ^{18}F [22, 23]. To our knowledge, the radiation absorbed dose of [^{18}F]fluoropaclitaxel has not been reported yet. Limited data on the biodistribution of [^{18}F]fluoropaclitaxel in humans [24], however, appeared to be comparable with the present biodistribution data of [^{11}C]docetaxel. Following intravenous administration of [^{18}F]fluoropaclitaxel, PET scans were performed in three healthy volunteers. High [^{18}F]fluoropaclitaxel uptake was observed in liver, gall bladder and intestine, whilst uptake in brain and lung appeared to be low. Seventy-five minutes after injection, [^{18}F]fluoropaclitaxel had been cleared from liver and subsequently excreted into intestine. When comparing biodistribution and pharmacokinetics of [^{18}F]fluoropaclitaxel and [^{11}C]docetaxel, it is important to realize that the chemical structure of [^{11}C]docetaxel is identical to that of clinically used, non-labelled docetaxel, whilst [^{18}F]fluoropaclitaxel is not identical to paclitaxel itself [22]. Introduction of a fluoride atom into the paclitaxel molecule effectively creates a different chemical structure and may result in a molecule with different pharmacokinetic and pharmacodynamic characteristics as compared to the paclitaxel molecule that is usually administered for the treatment of patients.

The present biodistribution results for [^{11}C]docetaxel are in line with three clinical observations in cancer patients who are treated with docetaxel. First, the extensive hepatic clearance of [^{11}C]docetaxel indicates that caution is warranted when treating patients with liver dysfunction. Indeed, in patients with clinical chemistry findings suggestive of mild to moderate liver function impairment [SGOT and/or SGPT > 1.5 × upper limit of normal (ULN), concomitant with alkaline phosphatase > 2.5 × ULN], total body clearance of the drug docetaxel is known to be lowered significantly. Second, [^{11}C]docetaxel uptake in bone marrow may mirror neutropenia, which was the dose-limiting toxicity in previous phase I clinical trials of docetaxel [25]. Third, [^{11}C]docetaxel uptake in brain was low. The blood-brain barrier is likely to be the major cause of this poor uptake. An important component of the blood-brain barrier is Pgp [26, 27], which acts as a drug efflux pump and for which docetaxel is a substrate [28]. This is reflected by the limited efficacy of systemic treatment with docetaxel for tumours or metastases in the brain [29]. In addition, Pgp-mediated efflux in the blood-testis barrier is known to maintain low drug concentrations in the testis [30]. Indeed, visual inspection of the [^{11}C]docetaxel PET images did not reveal any [^{11}C]docetaxel uptake in the testicular region, indicating that [^{11}C]docetaxel uptake in the testis is probably low.

Although not the primary aim of this study, [^{11}C]docetaxel uptake was also measured in tumours. Tumour uptake was highly variable, which may mirror differential sensitivity of tumours to docetaxel treatment. Studies with other radiolabelled anticancer agents such as [^{18}F]5-fluorouracil (FU) and [^{18}F]fluorotamoxifen [2] have shown that higher uptake of these radiolabelled agents in tumours appeared to be related to better tumour response. Radiolabelled anticancer agents could potentially predict treatment outcome and may contribute to individualized treatment planning. As patients in the present study were not scheduled to undergo docetaxel treatment, further studies are warranted to investigate whether tumour uptake of [^{11}C]docetaxel is predictive of outcome of docetaxel therapy. As background uptake of [^{11}C]docetaxel in the chest is low, it may be a useful tracer to predict docetaxel efficacy for tumours in the thoracic region, such as lung and breast cancer.

Conclusion

The highest uptake of [^{11}C]docetaxel was measured in gall bladder and liver, whilst uptake in brain and lung was very low. Administration of [^{11}C]docetaxel was safe with a mean effective dose of 4.7 μSv/MBq. [^{11}C]docetaxel uptake in tumours was moderate and highly variable between different tumours.

Acknowledgements The authors would like to thank Suzette van Balen, Amina Elouahmani, Judith van Es, Femke Jongsma, Rob Koopmans, Nassearah Sais and Annemiek Stiekema for scanning the patients, Henri Greuter, Kevin Takkenkamp and Robert Schuit for analysing the blood samples and Natasja Kok, Ilona Pomstra and Atie van Wijk for help with logistic planning and patient care.

Conflicts of interest None.

References

1. Van Oosterom AT, Judson I, Verweij J, Stroobants S, Donato di Paola E, Dimitrijevic S, et al. Safety and efficacy of imatinib (STI571) in metastatic gastrointestinal stromal tumours: a phase I study. Lancet 2001;358:1421–3.
2. Van der Veldt AA, Luurtsema G, Lubberink M, Lammertsma AA, Hendrikse NH. Individualized treatment planning in oncology:

role of PET and radiolabelled anticancer drugs in predicting tumour resistance. Curr Pharm Des 2008;14:2914–31.
3. Van der Veldt AA, Lammertsma AA, Hendrikse NH. [11C]docetaxel and positron emission tomography for noninvasive measurements of docetaxel kinetics. Clin Cancer Res 2007;13:7522–3.
4. Van Tilburg EW, Franssen EJ, Van der Hoeven JJ, Van der Meij M, Elshove D, Lammertsma AA, et al. Radiosynthesis of [11C] docetaxel. J Labelled Comp Radiopharm 2004;47:763–77.
5. Van Tilburg EW, Mooijer MP, Brinkhorst J, Van der Meij M, Windhorst AD. Improved and semi-automated GMP-compliant radiosynthesis of [11C]docetaxel. Appl Radiat Isot 2008;66: 1414–8.
6. Montero A, Fossella F, Hortobagyi G, Valero V. Docetaxel for treatment of solid tumours: a systematic review of clinical data. Lancet Oncol 2005;6:229–39.
7. Therasse P, Arbuck SG, Eisenhauer EA, Wanders J, Kaplan RS, Rubinstein L, et al. New guidelines to evaluate the response to treatment in solid tumors. European Organization for Research and Treatment of Cancer, National Cancer Institute of the United States, National Cancer Institute of Canada. J Natl Cancer Inst 2000;92:205–16.
8. Surti S, Kuhn A, Werner ME, Perkins AE, Kolthammer J, Karp JS. Performance of Philips Gemini TF PET/CT scanner with special consideration for its time-of-flight imaging capabilities. J Nucl Med 2007;48:471–80.
9. Hoekstra CJ, Hoekstra OS, Lammertsma AA. On the use of the injection catheter for venous blood sampling in quantitative FDG PET studies. Eur J Nucl Med 2000;27:1579.
10. International Commission on Radiological Protection. Report of the Task Group on Reference Man. ICRP Publication 23. New York: Pergamon; 1975.
11. Cristy M, Eckerman KF. Specific absorbed fractions of energy at various ages from internal photon sources. Oak Ridge: Oak Ridge National Laboratory; 1987.
12. Stabin MG, Sparks RB, Crowe E. OLINDA/EXM: the second-generation personal computer software for internal dose assessment in nuclear medicine. J Nucl Med 2005;46:1023–7.
13. International Commission on Radiological Protection. Limits for intakes of radionuclides by workers. ICRP Publication 30. New York: Pergamon; 1979.
14. International Commission on Radiological Protection. The 1990 Recommendations. Ann ICRP 1991;21:1–3.
15. International Commission on Radiological Protection. The 2007 Recommendations. Ann ICRP 2007;37:2–4.
16. Hirvonen J, Roivainen A, Virta J, Helin S, Någren K, Rinne JO. Human biodistribution and radiation dosimetry of 11C-(R)-PK11195, the prototypic PET ligand to image inflammation. Eur J Nucl Med Mol Imaging 2010;37:606–12.
17. International Commission on Radiological Protection. Radiological protection in biomedical research. ICRP Publication 62. New York: Pergamon; 1991.
18. FDA. Food and Drug Administration Code of Federal Regulations. 21 CFR 361–1. 1991.
19. Rosing H, Lustig V, Van Warmerdam LJ, Huizing MT, Ten Bokkel Huinink WW, Schellens JH, et al. Pharmacokinetics and metabolism of docetaxel administered as a 1-h intravenous infusion. Cancer Chemother Pharmacol 2000;45:213–8.
20. Liu N, Li M, Li X, Meng X, Yang G, Zhao S, et al. PET-based biodistribution and radiation dosimetry of epidermal growth factor receptor-selective tracer 11C-PD153035 in humans. J Nucl Med 2009;50:303–8.
21. Slifstein M, Hwang DR, Martinez D, Ekelund J, Huang Y, Hackett E, et al. Biodistribution and radiation dosimetry of the dopamine D2 ligand 11C-raclopride determined from human whole-body PET. J Nucl Med 2006;47:313–9.
22. Kalen JD, Hirsch JI, Kurdziel KA, Eckelman WC, Kiesewetter DO. Automated synthesis of 18F analogue of paclitaxel (PAC): [18F]paclitaxel (FPAC). Appl Radiat Isot 2007;65:696–700.
23. Kiesewetter DO, Jagoda EM, Kao CH, Ma Y, Ravasi L, Shimoji K, et al. Fluoro-, bromo-, and iodopaclitaxel derivatives: synthesis and biological evaluation. Nucl Med Biol 2003;30:11–24.
24. Kurdziel KA, Kalen JD, Hirsch JI, Wilson JD, Agarwal R, Barrett D, et al. Imaging multidrug resistance with 4-[18F]fluoropaclitaxel. Nucl Med Biol 2007;34:823–31.
25. Burris H, Irvin R, Kuhn J, Kalter S, Smith L, Shaffer D, et al. Phase I clinical trial of taxotere administered as either a 2-hour or 6-hour intravenous infusion. J Clin Oncol 1993;11:950–8.
26. Thiebaut F, Tsuruo T, Hamada H, Gottesman MM, Pastan I, Willingham MC. Immunohistochemical localization in normal tissues of different epitopes in the multidrug transport protein P170: evidence for localization in brain capillaries and cross-reactivity of one antibody with a muscle protein. J Histochem Cytochem 1989;37:159–64.
27. Thiebaut F, Tsuruo T, Hamada H, Gottesman MM, Pastan I, Willingham MC. Cellular localization of the multidrug-resistance gene product P-glycoprotein in normal human tissues. Proc Natl Acad Sci U S A 1987;84:7735–8.
28. Fojo T, Menefee M. Mechanisms of multidrug resistance: the potential role of microtubule-stabilizing agents. Ann Oncol 2007;18:v3–8.
29. Sanson M, Napolitano M, Yaya R, Keime-Guibert F, Broët P, Hoang-Xuan K, et al. Second line chemotherapy with docetaxel in patients with recurrent malignant glioma: a phase II study. J Neurooncol 2000;50:245–9.
30. Bart J, Groen HJ, Van der Graaf WT, Hollema H, Hendrikse NH, Vaalburg W, et al. An oncological view on the blood-testis barrier. Lancet Oncol 2002;3:357–63.